Journal of the Meteorological Society of Japan, Vol. 73, No. 5, pp. 909–923, 1995

Interannual Variations of Summer Precipitation in the Arid/semi-arid Regions in China and Mongolia: Their Regionality and Relation to the Asian Summer Monsoon

By Akiyo Yatagai[1] and Tetsuzo Yasunari

Institute of Geoscience, University of Tsukuba, Ibaraki 305, Japan

(Manuscript received 10 April 1995, in revised form 17 August 1995)

Abstract

In this study, interannual variations of summertime precipitation over arid and semi-arid regions in China and Mongolia are investigated. To clarify the regionality of the interannual variability in summer precipitation, an analysis technique of rotated empirical orthogonal functions is applied for a recent 40-year (1951–1990) period of summer precipitation. As a result of the REOF, five regions have been determined: I) Taklimakan Desert, II) Loess Plateau, III) North China to central and the southeastern part of Mongolia, IV) the north of Tianshan Mountains, and V) the northern part of Mongolia. Summertime precipitation over Region III) shows a significant decreasing trend after 1955.

Next, to examine how the variations in precipitation in these regions are influenced by the Asian (Indian) summer monsoon activity in the mid-latitudes, correlations with all-India monthly and seasonal rainfall (IMR) are investigated. Further, the change of atmospheric circulation patterns with the interannual variation of summer precipitation of Regions I and II are also examined. The results are summarized as follows:

1) The interannual variation of summer precipitation of Region I (Taklimakan Desert) is mainly related to the windward mid-latitude circulation and eastward (westward) shift of the Tibetan High in a wet (dry) year. This region shows a clear negative correlation with IMR in June and July, and the relationships are caused by a rather local circulation change with IMR variation over Central Asia.

2) In Region II (Loess Plateau, the middle reaches of Yellow River), interannual variation of summer precipitation shows a positive correlation with IMR through the summer monsoon season. It shows a clear 2–3 year periodic oscillation, and seems to be closely related to the atmosphere/ocean interaction in the equatorial Pacific.

1. Introduction

Desertification is one of the serious problems in the current global environment. The prevailing definition of "desertification" by the United Nations Environmental Programme (UNEP) is "Land degradation in the arid, semiarid and dry sub-humid areas resulting mainly from adverse human impact" (UNEP, 1992), which emphasizes the irreversibility of land resoures. However, to grasp the current trend and variabilities of water balance, especially rainfall, is indispensable for understanding the mechanism of desertification and combating desertification. Recently intensive observational researches have been made in the arid and semi-arid regions in China, for example, around the Heihe River Basin (the Heihe River Field Experiment, HEIFE) and Taklimakan Desert (Japan-China Joint Research Project on the Mechanism of Desertification). However, few studies have been conducted on climatic variation of that region, especially related to the large-scale circulation.

In terms of "desertification", trend or long-term variability of precipitation seems to be essential. A recent precipitation trend over China and Mongolia was reported by Yoshino and Aoki (1986), Chen *et al.* (1991), Chen *et al.* (1992) and Yatagai and Yasunari (1994). Chen *et al.* (1992) pointed out that during the past 40 years (1951–1990), especially in the 1980s, China has generally been drying out. Yatagai and Yasunari (1994) showed a significant decreasing trend (1951–1990) of summer precipitation over North and South China and the middle part of Mongolia, while significant increasing trend

1 Present affiliation: National Space Development Agency of Japan Earth Observation Research Center (EORC)

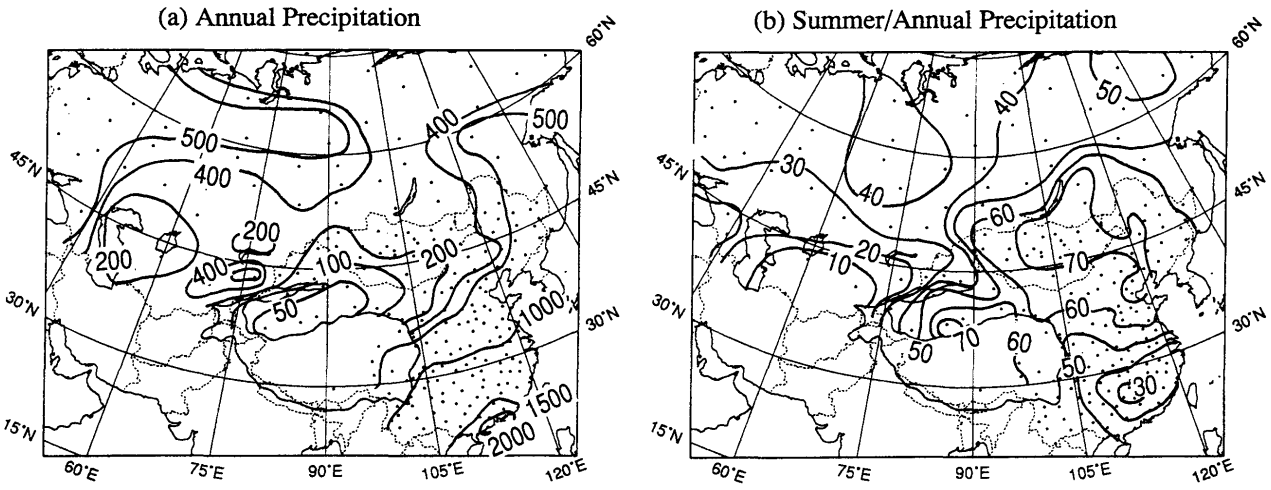

Fig. 1. (a) Geographical distribution of mean (1951–1990) annual total precipitation (mm), and (b) the ratio (%) of summer (JJA) precipitation to annual total precipitation. Dots indicate the station network used here.

was evident over some stations around the Taklimakan Desert. They also investigated the decadal-scale oscillation of summer precipitation over China and Mongolia and its relation to Northern Hemispheric circulation changes.

Understanding the nature of short-term precipitation variability is essential for assessing and coping with desertification. Tian and Yasunari (1992) and Shen and Lau (1995) focused on the importance of the 2–4 years oscillation over China, and examined the relationship of the oscillation to the summer monsoon and tropical SOI (Southern Oscillation Index) or SST (Sea Surface Temperature). However, few studies have focused on the arid and semi-arid region of China and Mongolia from the global or hemispheric point of view, which should provide important basic information for understanding desertification. Wang and Li (1990) examined the precipitation variation over the Loess Plateau in China and its association with El Niño/Southern Oscillation (ENSO); however, its physical mechanism or circulation fields are not fully investigated. Besides, their study did not include the variability in adjacent arid and semi-arid regions.

Meanwhile, the relationship between the Chinese and Indian summer (June to September) monsoon rainfall has already been examined using a 30-year (1951–1980) data set (Guo and Wang, 1988; Chen *et al.*, 1992; Kripalani and Singh, 1993). These studies pointed out a significant positive correlation in some regions of North China, while a negative correlation existed in a part of Tibet and Xinjiang. Although these researches pointed out statistical relationships between the rainfall in China and the Indian summer monsoon, atmospheric circulation fields associated with these relationships have not been clarified yet.

Moreover, since precipitation of the arid and semi-arid region over China and Mongolia is considered to be affected both by the monsoon circulation and mid-latitude westerly disturbance, the interannual variability of summer precipitation may be different from area-to-area as well as from season-to-season. Therefore, in this study, we deal with the large arid/semi-arid areas distributed in the eastern part of the Eurasian continent, and deduce the regional divisions of interannual variation of summer precipitation, based upon the different characteristic natures of the variabilities. The correlations of variations of precipitation in these regions and the Asian (Indian) summer monsoon activity are also examined based on the all-India monthly and seasonal rainfall (IMR). Finally, the atmospheric circulation patterns associated with the regional variations are also presented.

The regional division is presented in Section 3. The relationship with IMR is dealt with in Section 4. Discussion, especially on the atmospheric circulation, is in Section 5. A summary follows in Section 6.

2. Data and method of analysis

2.1 Data

The following data sets were used in this study.

(1) Monthly precipitation data at 160 stations over China for 40 years (1951–1990) compiled by the State Meteorological Administration of China;

(2) Monthly precipitation data at 23 stations over Mongolia for 40 years (1951–1990) compiled by the Ministry for Nature and Environment of Mongolia;

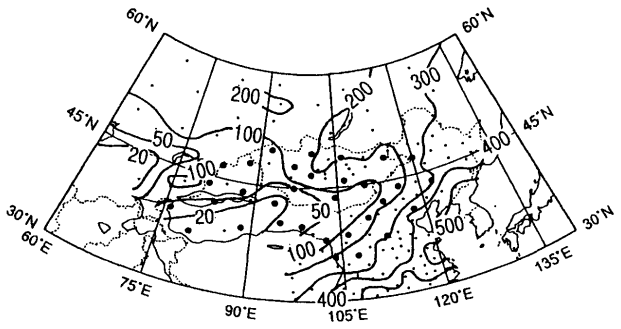

Fig. 2. Geographical distribution of mean (1951–1990) summer (JJA) precipitation (mm). Large circles are the 32 stations selected for REOF analysis.

(3) Monthly precipitation data at 85 stations over the former USSR compiled by the National Center for Atmospheric Research (NCAR) (1951–1988) and from Monthly Climatic Data for the World (1989–1990);

(4) All-India monthly rainfall data (1951–1990) adopted from Parthasarathy *et al.* (1994).

(5) Monthly mean sea-level pressure (SLP), and 500 and 100 hPa geopotential height on 10°longitude/latitude grid in the Northern Hemisphere, compiled by the Japan Meteorological Agency (1951–1990, but 1963–1990 for 100 hPa).

The names of major geographical regions used in this study can be seen in Fig. A1. China's present administrative units and traditional divisions can be found in the Appendix of Yatagai and Yasunari (1994).

Figure 1a shows the spatial pattern of mean (1951–1990) annual total precipitation over China, Mongolia and Asian part of the former USSR. The least precipitation is apparent over the Taklimakan Desert in this area. Relatively large precipitation is noted on the northwest side of Tianshan Mountains. The ratio of summer (June, July and August, hereafter referred to as JJA) precipitation to the annual precipitation reveals clear contrast between the west and the east of the Tianshan Mountains (Fig. 1b). In the central Asia between the Caspian Sea and the Tianshan Mountains, summertime rainfall is relatively small. In contrast, a large fraction of rainfall appears in summer to the east of Tianshan and Pamir. In most parts of Mongolia and North and Northwest China, except for the north of the Tianshan mountains, more than 50 % of the annual total precipitation occurs in summer. Especially, to the north of the Tibetan Plateau and in most parts of Mongolia, summer precipitation occupies more than 70 % of annual precipitation.

In this study, we focused on the interannual variation of summer precipitation over arid/semi-arid region in North and Northwest China and Mongolia, where a large portion of precipitation occurs in summertime, as shown in Fig. 1b. Figure 2 represents the mean JJA precipitation. The region with JJA precipitation amounts less than 300 mm/(92days) is referred to as the arid and semiarid region here. The region roughly consists of desert (BW) and steppe (BS) climates by the Köppen climate classification category. The station network examined for the regionality of the interannual variability of summer precipitation is also displayed in Fig. 2.

2.2 Method of analysis

First, we investigate the interannual variation of the JJA precipitation over the arid and semi-arid regions by applying the rotated empirical orthogonal function (REOF) analysis. The (un-rotated) empirical orthogonal function (EOF) analysis is often used to examine the time-space structure of climatic data, and it was applied to identify climatic divisions (*e.g.*, Gadgil and Joshi, 1983; Yoshino and Chiba, 1984). However, REOF analysis has been shown to be more useful for deducing the regionality of climatic factors (*e.g.*, Richman and Lamb, 1985) and climatic divisions (*e.g.*, Murata, 1990; Nishimori, 1994), because it has advantages in obtaining localized modes for the full domain. The mathematical procedure and benefits of REOF analysis and application to meteorology or climatology has been intensively discussed by Horel (1981) and Richman (1986), among others. In this study, a REOF refers to a linear transformation of the initial EOFs utilizing the varimax method. The varimax method is one of the techniques for orthogonal rotation that maximizes the total variance of the squared sum of elements of factor loadings for each component. After the rotation a factor loading will have localized elements with few large values among many smaller values. Hence the rotation of the principal components using the varimax method increases the discrimination among the loading and makes them easier to interpret (Ladd and Driscoll, 1980).

Here the 32 stations are selected for the REOF analysis with a relatively uniform distribution of the station network (Fig. 2). First, the JJA precipitation time-series are normalized by taking cubic roots of original precipitation to approximate the sample histograms to the Gaussian distribution. Then a correlation matrix of the variables is used for computing the eigenvalues and eigenvectors of EOFs, since this study aims at the interannual variability of the precipitation not at that of the absolute amount. After that, the first five EOFs are orthogonally rotated considering the number of variables and regional scale. Therewith regional characters of interannual variation of summer precipitation are

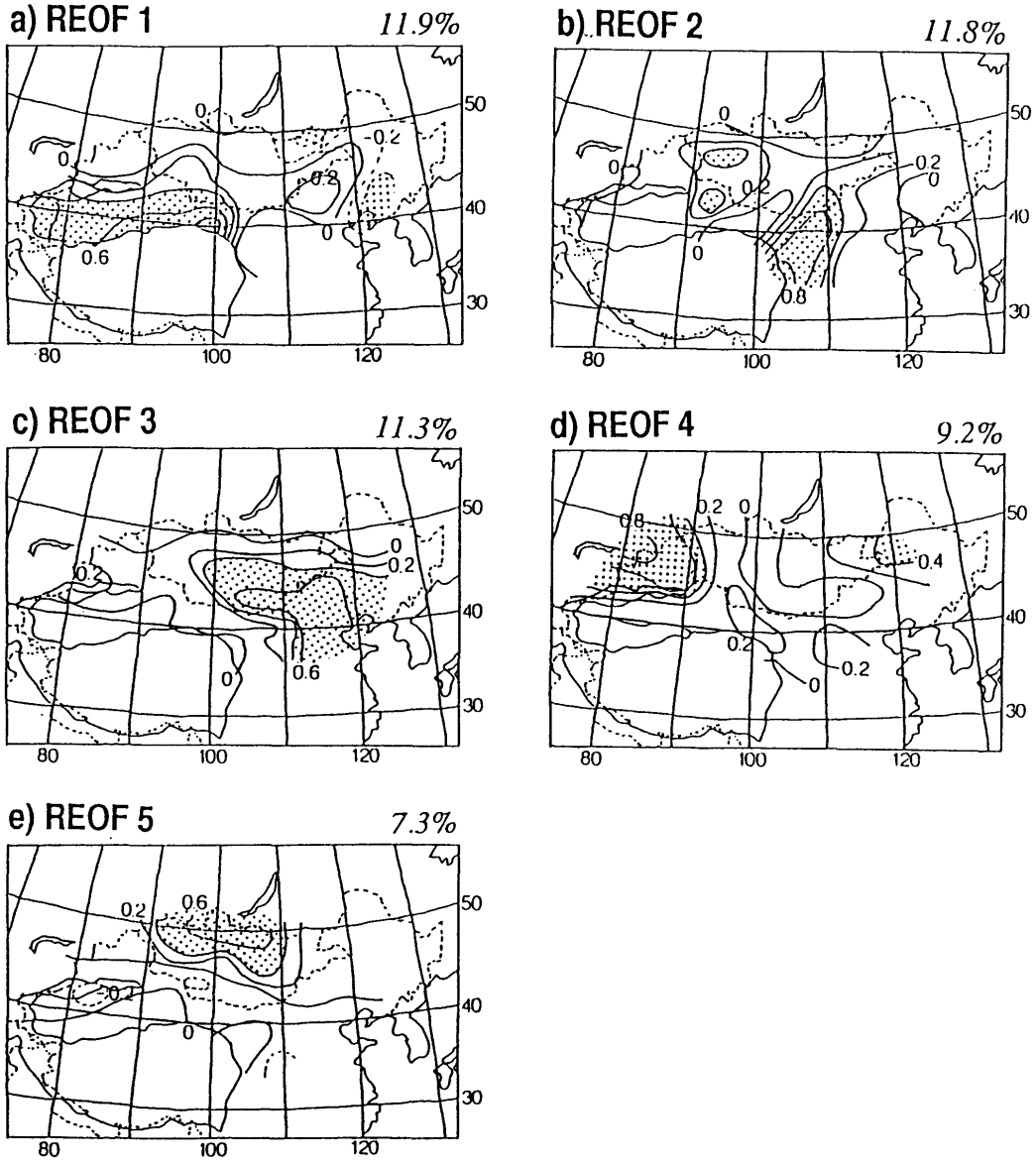

Fig. 3. Factor loadings of the first five REOFs of summertime (JJA) precipitation anomalies. The contour interval is 0.2; contours for the negative values are shown with dashed lines. Dotted areas indicate the regions with the values exceeding 0.4. The contribution to the total variance (%) for each component is presented at the upper right of each panel.

described.

In Section 4, the relationship of interannual variation of the arid and semi-arid regions with Indian Monsoon Rainfall (IMR) is examined. Cubic roots of the original precipitation data are computed before correlation coefficients of the precipitation variation are obtained.

3. Time and space structure of interannual variability

3.1 Regional divisions by REOF analysis

Figure 3 shows the factor loading patterns of the dominant five components. The contribution of each components (after rotation) to the total variance is also shown in Fig. 3. The first five components account for 51.5 % of total variance. Dotted area indicates the area of factor loading values exceeds 0.4 (or below −0.4). Since factor loading designates correlation coefficients between time series of each stations and score, the dotted areas correspond to the correlation coefficients with 1 % significant (or less) level (0.403). The time sequence of the score for each REOF is presented in Fig. 4 (thick solid line).

Based on the factor loading pattern of each component, the five regions are delineated as shown in Fig. 5. The contour lines of 0.4 (−0.4) of each factor loading pattern has demarcated these sub-regions almost exclusively. If a station had significant factor

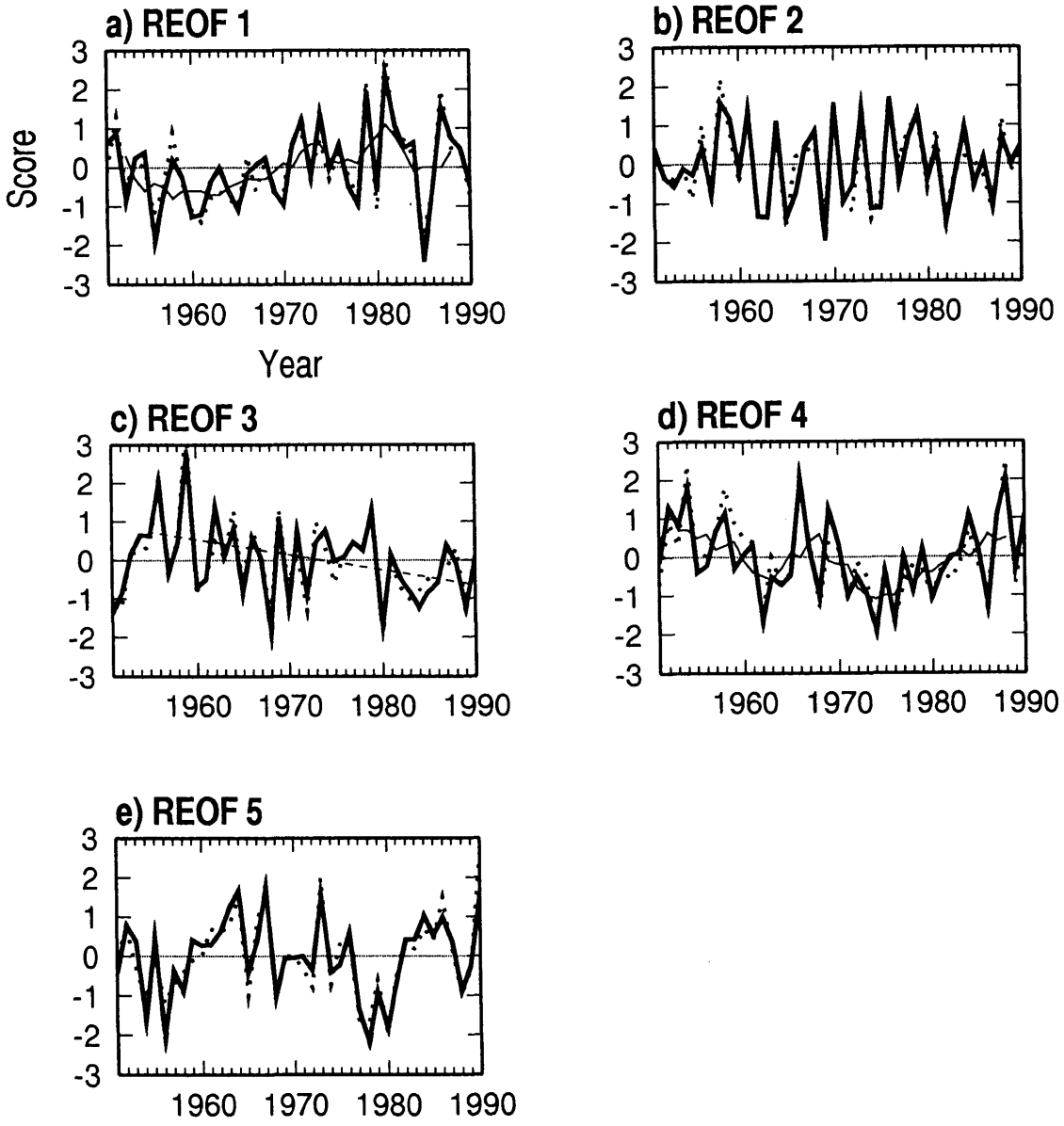

Fig. 4. Time series of the factor scores (non-dimensional values) of the REOFs 1 to 5 are shown in (a) to (e), respectively, with thick solid lines. The standardized original JJA precipitation series averaged for each corresponding region is also shown with a dotted line. Five-year running mean scores of REOFs 1 and 4 are added in (a) and (d), respectively, with thin lines. As for REOF 3, the linear trend of the original JJA precipitation after 1955 is indicated with a thin dashed line.

loadings in any two of loading patterns, the station was included to the Region where the station showed higher loading value in the corresponding component. A few significant stations isolated from the main regions are excluded from this regional division. Hereafter, the sub-regions deduced from these REOFs are referred to as Regions I to V, respectively.

The secular variations of area-average precipitation for the respective regions (displayed in Fig. 5) are standardized and also presented in Fig. 4 (dotted line). It is obvious that the scores coincide with the regional precipitation very well. The correlation coefficient between the score and the regional precipitation in each region is more than 0.9 for all components (which will be shown in Table 2).

We describe the characteristics of each divided region and the scores. Region I shows the variability of Taklimakan Desert and a part of Gobi Desert, surrounded by Tianshan, Pamir and Tibetan Plateau. A decadal-scale oscillation is seen in this component drawn as a thin lined curve in Fig. 4a. In the last ten years, the year-to-year amplitude is large, with the maximum in 1981 and minimum in 1985. It is in-

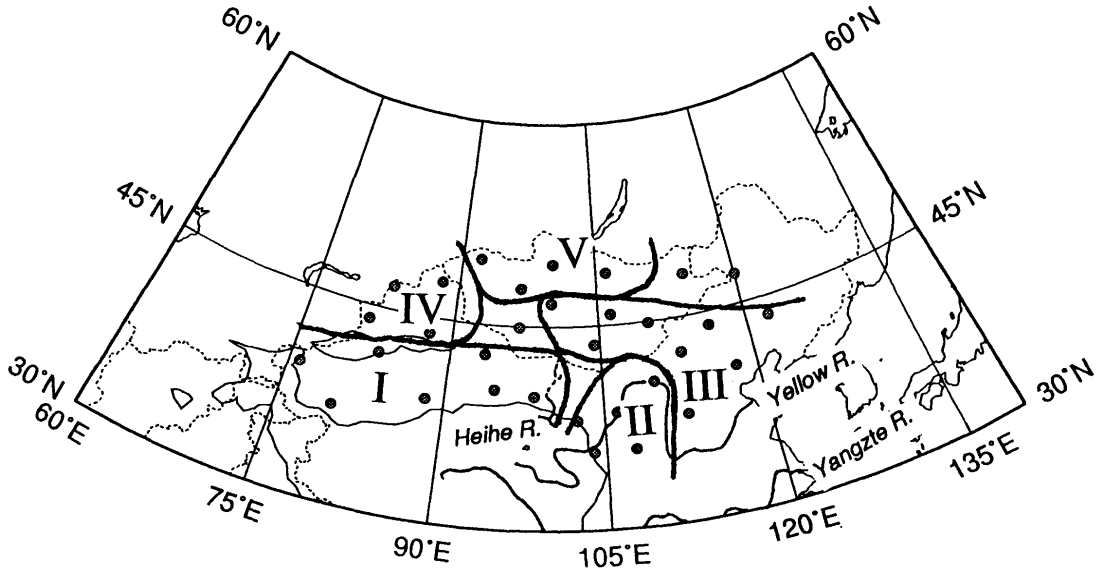

Fig. 5. Five sub-regions (Region I to V) deduced from JJA REOF analysis. Heihe River, Yellow (Huanghe) River, and a part of Yangtze (Chang Jiang) River are also drawn.

triguing that the Heihe River Basin (HEIFE region) is located in the easternmost part of this region, adjacent to Region II.

Region II corresponds to the horseshoe-shaped arc region of the middle reach of the Yellow River in Nei-Mongol, which encircles the Ordos Plateau and a part of the Loess Plateau. The time series of interannual variation of summer precipitation of this region (Fig. 4b) shows a clear 2–3 years periodic oscillation. As for Region II, Wang and Li (1990) also pointed out the following features: 1) a 2–3 year quasi-periodic fluctuation and 2) a tendency for rainfall deficiency during El Niño/Southern Oscillation years, and so on. The details of the correlation with IMR will be discussed in Section 4.

Region III corresponds to a wide area spreading from North China to the southeastern and central part of Mongolia. An apparent decreasing trend is seen in the interannual variation of summer precipitation of this region (Fig. 4c). After 1955 to 1990, the regional mean precipitation of this area shows a decreasing linear trend with a 99 % confidence level, denoted by a thin line in Fig. 4c. This result agrees with that of Yatagai and Yasunari (1994), which depicted the significant decreasing trend of JJA precipitation over this region from 1951 to 1990. The present result has shown that the actual decreasing tendency started in the late 1950s.

Figures related to Region IV (Figs. 3d, 4d) represent the interannual variation of summer precipitation to the north of the Tianshan mountains and the northernmost part of Nei Mongolia. The time series of this component shows a strong decadal-scale variability, as shown by a thin line in Fig. 4d.

Region V (Fig. 3e) is located in the northern part of Mongolia. The time series (Fig. 4e) does not show any systematic oscillation nor trend in this period (1951–1990).

3.2 The contribution of June, July and August precipitation to the scores

In the previous sub-section, the regional division was done for JJA precipitation, without considering the intra-seasonal or month-to-month changes. However, the atmospheric circulation changes quite substantially within the summer months in East Asia. Thus, information on monthly contributions will be necessary, especially in the context of the relationship to the atmospheric circulation field discussed in the following sections (Section 4 and 5).

Table 1 indicates the 40-year mean monthly and JJA precipitation for each region. In July, Region I (Taklimakan Desert) , Region III (where the decreasing trend was detected) and Region V (the northern part of Mongolia) receive the most precipitation among the three months. On the other hand, in Region II (Loess Plateau), precipitation is a maximum in August, and in Region IV (north of Tianshan Mountains), precipitation in June provides the maximum in the summer three months.

Table 2 shows the correlation coefficients between the scores of REOFs and the regional precipitation of each month and season (JJA). As mentioned before, each score represents the regional JJA precipitation for each dominant region very well with correlation coefficients of more than 0.9. The highest correlation value among the three months appears to be the month with the maximum precipitation, except for Region IV. Other than for Region II (Loess Plateau), the largest correlation coefficient is found

Table 1. Regional mean JJA precipitation (mm).

Month	Region I Taklimakan	Region II Loess P.	Region III Decreasing	Region IV N.Tianshan	Region V N.Mongolia
June	8.3	38.2	43.9	28.1	41.3
July	10.3	71.6	78.8	25.1	62.4
August	7.5	78.2	68.9	16.2	50.5
JJA	26.1	188.0	191.6	69.4	154.2

Table 2. The correlation coefficients between scores and regional monthly, JJA precipitation.

Month	Region I Taklimakan	Region II Loess P.	Region III Decreasing	Region IV N.Tianshan	Region V N.Mongolia
June	0.513	0.517	0.610	0.507	0.574
July	0.776	0.454	0.720	0.725	0.663
August	0.524	0.843	0.614	0.216	0.598
JJA	0.942	0.928	0.940	0.901	0.929

Table 3. The correlation coefficients between monthly regional precipitation and IMR. *: the 5 % significance level. **: the 1 % significance level.

Month	Region I Taklimakan	Region II Loess P.	Region III Decreasing	Region IV N.Tianshan	Region V N.Mongolia
June	−0.355*	0.306	0.168	−0.016	0.151
July	−0.316*	0.328*	0.300	−0.003	−0.317*
August	0.040	0.327*	0.298	0.348*	0.175
JJA	−0.342*	0.454**	0.232	0.118	−0.016
Score	−0.397*	0.367*	0.137	0.019	−0.050

in July. The largest coefficient is in August in Region II. A remarkably low correlation coefficient is found in August for Region IV (north of Tianshan M.).

4. Relation between precipitation of the arid/semi-arid region and the Indian monsoon

Here we investigate the correlation between monthly IMR and regional averaged precipitation deduced in Section 3. Table 3 shows the correlation coefficients between IMR and the regional mean precipitation for June, July, August, JJA and scores. Region I (Taklimakan Desert) shows a significant (exceeding 5 % level) negative correlation coefficient in June, July and also JJA total rainfall, while it does not show significant correlation in August. In Region II, the correlation coefficient of JJA total precipitation is positive, exceeding the 1 % significant level. All monthly correlation coefficients show significant relations to IMR, though that of June is slightly below the 5 % level.

Both the score and the regional mean precipitation of Region III are relatively high, but do not attain a significant level (Table 3). The August precipitation in Region IV and the July precipitation of Region V show significant positive/negative correlation coefficients, though there are no correlations of JJA precipitation for Region IV and V with that of IMR.

If we compare Table 3 with Table 1 and 2, it can be seen that the month when the precipitation strongly contributes to the interannual variation of summer precipitation does not always show a large correlation coefficient with IMR. In Region IV, for example, a significant correlation with IMR is detected in August, when the precipitation amount is relatively small and is not correlated to the seasonal mean precipitation.

Figures 6a,6b depicts the relation between the score of REOF I/II and IMR (JJA) in scatter diagrams. The negative and positive correlation of IMR (JJA) with scores I and II are confirmed by these figures, respectively. ENSO years, denoted by circles, are defined by the Southern Oscillation Index (SOI) anomaly in summer. Score II, which represents the interannual variation of summer precipitation in Region II, shows that a relatively dry condition prevails in ENSO years, except in 1976. Since Waker

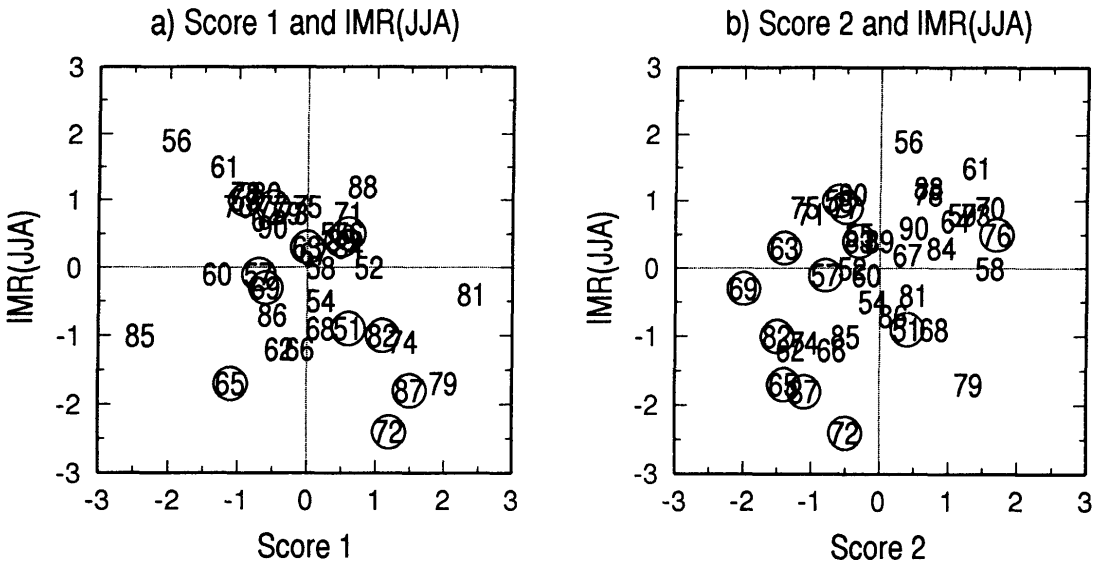

Fig. 6. (a) Scatter diagrams of the relation between scores of (a) REOF 1 and IMR (JJA), and (b) scores of REOF 2 and IMR (JJA). Both values are standardized. Numbers plotted in the diagram represent the year minus 1900. Circles which surround the numerals denote ENSO years.

and Bliss (1932), many studies have documented the coupling system of the Indian summer monsoon and ENSO phenomena (*e.g.*, Yasunari, 1990). This result not only agrees with that of Wang and Li (1990), but also suggests that the interannual variation of summer precipitation of Region II is affected by the coupling system of Indian monsoon and Atmospheric/Ocean interaction system.

On the other hand, the score of REOF I seems not to show any relation with ENSO years. That is to say, both the scores of REOFs I and II show significant correlation with IMR, only the score of REOF II reveals a relation with ENSO phenomena. To inquire further into these relations, the change of atmospheric circulation anomalies associated with these two modes and also with IMR will be displayed in the next section.

5. Atmospheric circulations relevant to regional precipitation

It has been revealed that Heihe River Basin is situated in the easternmost part of Region I, adjacent to Region II. Interestingly, Regions I/II have significant negative/positive correlations with IMR. So we examine here the atmospheric circulation patterns correlated with the precipitation of Region I and II.

Figures 7a–7c show the correlation patterns between the score of REOF 1 and (a) 100 hPa height, (b) 500 hPa height and (c) SLP anomalies, respectively, over the Northern Hemisphere north of 20°N. Since we have elucidated that the interannual variation of summer precipitation of Regions I is largely affected by those of July, we also show the correlation patterns for July, as shown in Figs. 7d–7f. The shaded (hatched) area indicates the area with positive (negative) correlation coefficient with a 5 % significance level. The patterns of Figs. 7 a–7c and 7d–7f are very similar to each other, though some minor differences are noticed.

In the 100 hPa correlation pattern (Fig. 7d), the significant positive correlation coefficient is noticeable over Central and South China, which indicates that the Tibetan High is intensified in its eastern part, when relatively more precipitation occurs in Region I. The same feature is apparent in Fig. 7a, though it is not so significant. This feature is confirmed by the 100 hPa height composite charts, shown in Fig. 8a and 8b, for wet/dry years based on the positive/negative July precipitation values exceeding the unit (standard deviation) values. In wet years (Fig. 8a), the Tibetan high depicts two centers at its eastern part (around 100°E/30°N) and at its westernmost part (50°E/35°N). On the other hand, in the dry year in Region I (Fig. 8b), it is centered in the western part of the Plateau (70°E/30°N) and its eastern part is very weak.

In the 500 hPa patterns (Fig. 7b and 7e), zonally-oriented significant positive correlations appear in the mid latitudes, that is to say, over the eastern part of America, north of Europe, around the Ural mountains, and around Lake Baikal. Over the Taklimakan Desert and Atlantic Sea, a negative correlation is seen. The composite pattern of the wet years for Region I in July (Fig. 8c), demonstrates that the mid-latitude trough locates around 90°E/~40°N and a slack ridge is located in Central Asia. In the dry years (Fig. 8d), the troughs extends along 45°E and around 110°E and relatively zonally over the

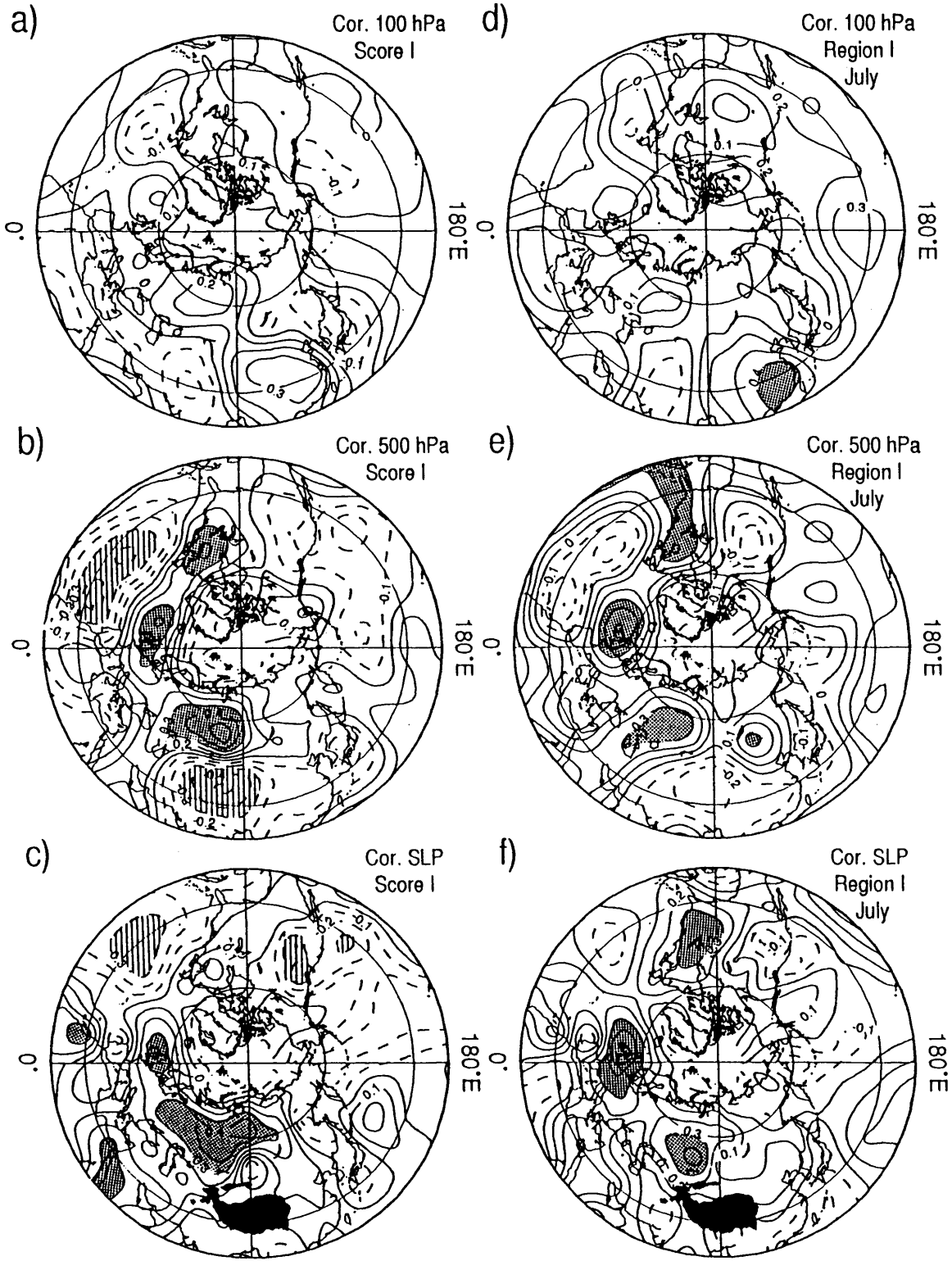

Fig. 7. Correlation coefficients between the score of REOF 1 and the anomalies of (a) 100 hPa height, (b) 500 hPa height and (c) SLP. The contour interval is 0.1. Solid (dashed) lines show positive (negative) values. Shaded (hatched) area indicates the region with the positive (negative) correlation coefficients beyond the 5 % significant level. (d)–(f) are same as (a)–(c), respectively, but for July precipitation of Region I.

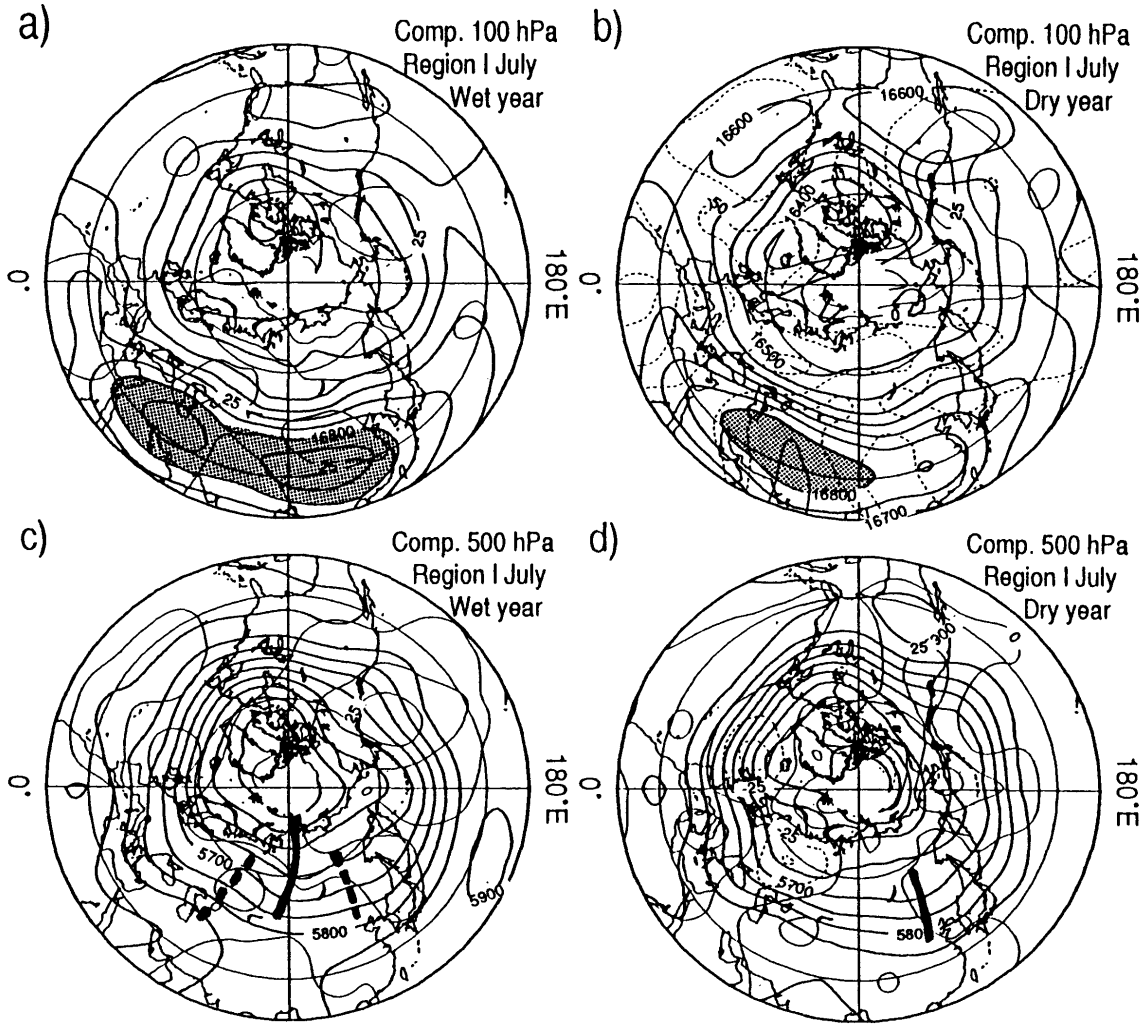

Fig. 8. Composite height charts at 100 hPa for the years of (a) more than the unit value of precipitation, and (b) less than the unit value, for July in Region I (Thick lines). The contour intervals are 50 gpm. Shaded areas correspond to the area where the geopotential height is greater than 16800 gpm. Thin solid (dashed) lines indicate positive (negative) anomalies of geopotential height. The contour intervals for anomalies are 25 gpm. (c) and (d) show the same charts as (a) and (b), but for at 500 hPa height. Thick solid/dashed lines indicate the trough/ridge positions over the Eurasian Continent.

Taklimakan Desert. The correlation coefficient pattern of SLP (Fig. 7c,7f) is very similar to that of 500 hPa (Fig. 7b,7d).

These overall features suggest that the northward/southward shift of the mid-latitude westerly circulation on the windward side (to the west of Region I) and the eastward/westward shift of the Tibetan High seem to be associated with the interannual variation of summer precipitation of Region I.

Figure 9 shows the same correlation coefficient charts but for Region II and in August (d–f). Remarkably different patterns are apparent from that of Region I. The correlation patterns for Region II in August (Fig. 9d–9f) seem to be more clear than those of the score of REOF II (Fig. 9a–9c). In the 100 hPa correlation pattern for August (Fig. 9d), significant positive correlations are shown over North and Central China, east of the Caspian Sea and northern Africa, which implies that the Tibetan High extends in the northeastern and northwestern part of itself when Region II has relatively more rain in August. These features suggest that the horizontal (east-west) scale of the Tibetan High is larger in the wet years than in normal or dry years for Region II. The positive correlation over North and Central China is also apparent in the corresponding 500 hPa correlation pattern (Fig. 9b,9e). The large significant positive correlation is noticeable over the North Pacific (in August), which suggest westward expansion (or retreat) of the North Pacific High associated with more (or less) precipitation in Region II. Neg-

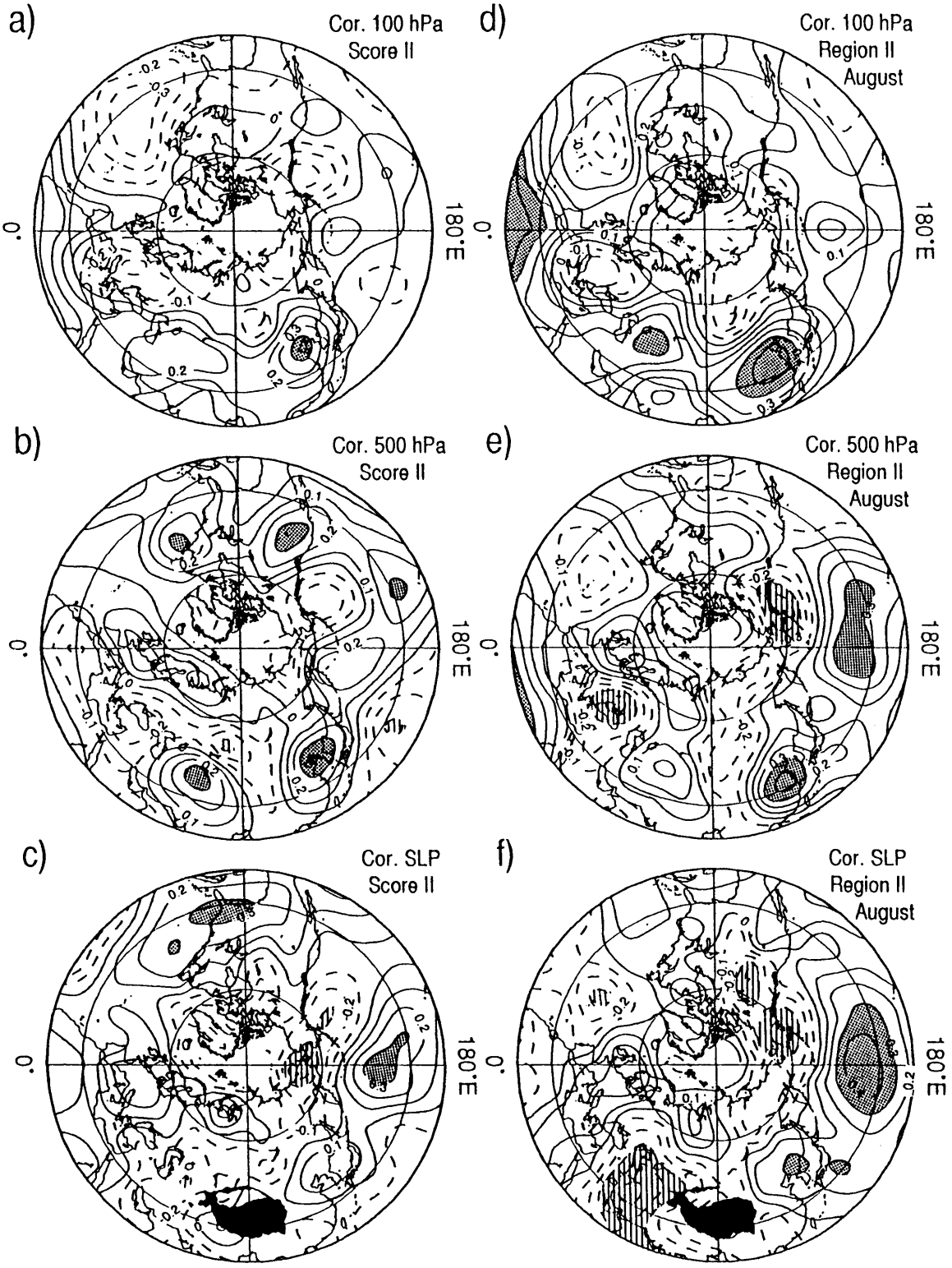

Fig. 9. (a)–(c) Same as Figs. 7a–7c but for a score of 2, respectively. (d)–(f) Same as Figs. 8d–8f, respectively, but for Region II in August.

ative correlation is distributed around the Aleutian both at the 500 hPa and SLP levels. Significant negative correlations are notable around Iran and Caspian Sea in the SLP field, and around Black Sea in the 500 hPa field in August, which likely to be related to IMR (Tanaka, 1983; Yasunari, 1986).

For comparison, we reproduced the correlation patterns between IMR and a) 100 hPa, b) 500 hPa

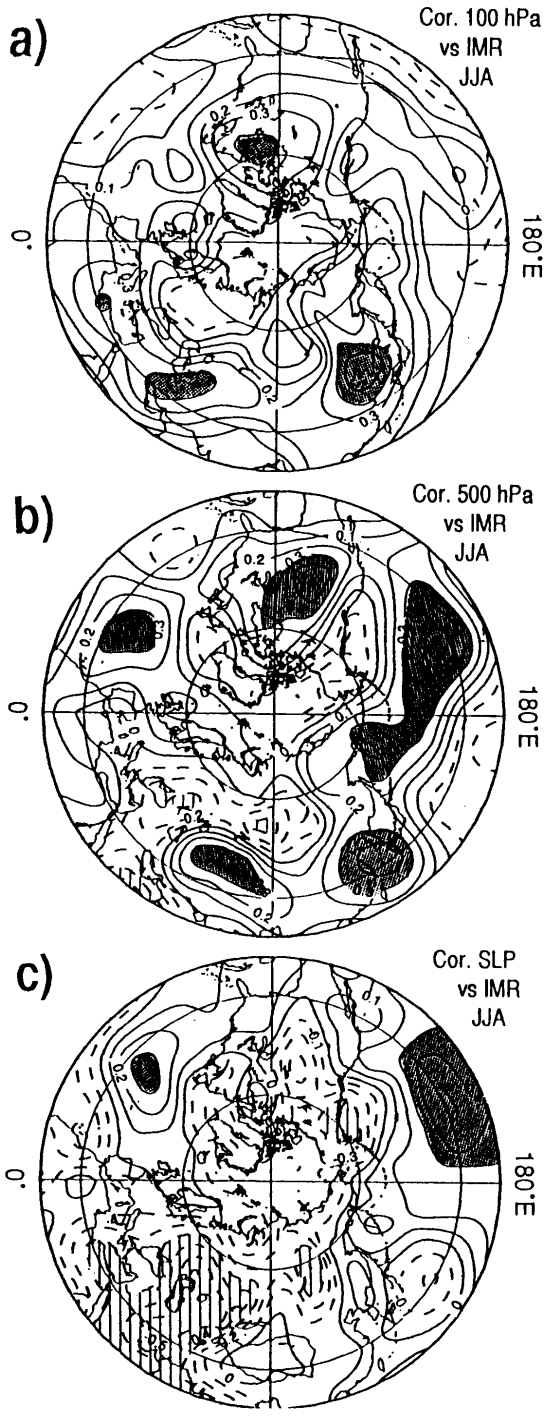

Fig. 10. Correlation coefficients between IMR in JJA and the anomalies of (a) 100 hPa height, (b) 500 hPa height, and (c) SLP. Details are the same as those in Fig. 7.

height and c) SLP as shown in Fig. 10. They are very similar to the patterns of Fig. 9d–9f. It has been noted that IMR is closely related with the expansion of the Pacific High, pressure around the Aleutian islands, and the east/west extension of the Tibetan High. Thus the interannual variation of IMR also seems to be important for summer precipitation for Region II, especially in August through the variations of these systems.

For east Asia, the existence of a quasi-biennial oscillation, and its relation with the Indian summer monsoon or ENSO on this time scale have been noted (Wang and Li, 1990; Lau, 1992; Tian and Yasunari, 1992; Shen and Lau, 1995). In Sections 3 and 4, summer precipitation of Region II shows: 1) a 2–3 year quasi-periodic fluctuation, 2) significant positive correlation with IMR, and 3) a tendency for less precipitation during ENSO years. The correlation patterns relevant to Region II and IMR seem to confirm the above results. Namely, the precipitation in this region seems to be strongly affected by the 2–3 year periodic fluctuation attributed to the atmosphere/ocean interaction system.

In contrast, Region I is attributed to the circulation variability over the north Atlantic through Central Asia. There are no common correlation patterns between Fig. 7 and Fig. 10, except for those over Central Asia which is adjacent to Region I. Raman and Rao (1981), Tanaka (1982,1983), and others, pointed out that break monsoon in India is preceded by the blocking high in west Asia, north of the Caspian Sea. For further study concerning this rather local system over Central Asia affecting the summer precipitation variation in Region I, the interaction between the active-break cycle of Indian monsoon and mid-latitude circulation should be taken into consideration in the future.

This section clarified that Region I and II are affected by the anomalies which show rather different general circulation systems, nevertheless both regions show significant negative/positive correlation with IMR. Namely, in Region I, the interannual variation of summer precipitation is influenced by the changes in the windward westerly circulation over the Atlantic through Central Asia, and it is correlated with Indian monsoon circulation as the rather local change over Central Asia. On the other hand, the interannual variation in Region II is directly associated with the large-scale Indian summer monsoon and the coupled atmosphere/ocean system in the Pacific.

6. Summary and remarks

This study has presented the time-space structure of the interannual variation of summer precipitation in the arid and semi-arid regions in China and Mongolia using data over 40 years (1951–1990). First, the regional divisions were deduced over these regions by applying the REOF analysis, and five regions were identified. Secondly, the relation of their interannual variability to the Indian monsoon rainfall (IMR) was examined for each summer month as well as for the whole summer season (JJA). Thirdly, the atmospheric circulation patterns in the North-

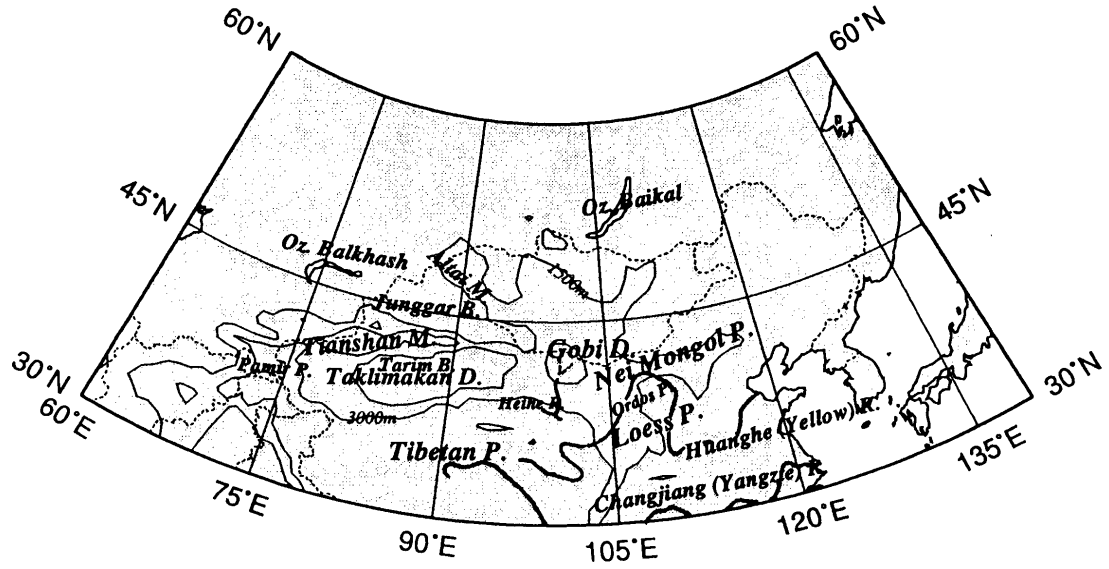

Fig. A1. Geography of the arid/semiarid regions over China and Mongolia. D.: Desert, M.: Mountains, P.: Plateau and R.: River. Solid contours represents altitudes of 1500 and 3000 m.

ern Hemisphere related to the interannual variation of summer precipitation of the first two regions were investigated.

The results are summarized by each region as shown below:

1) Over Taklimakan Desert (Region I), including the Heihe River Basin (HEIFE region), the interannual variation of summer precipitation shows strong decadal-scale oscillation, and its amplitude is relatively large after 1980. The variation of this region is related to the changes in the westerly circulation, which shows extension of the mid-latitude trough in wet years. The Tibetan High is strengthened (weakened) in its eastern part in wet (dry) years. The regional representative precipitation shows clear negative correlation with IMR in June and July. The relation with IMR is caused through a rather local circulation change over Central Asia.

2) Over a part of the Loess and Ordos Plateaux, the middle reaches of Yellow River (Region II), a periodic oscillation with a period of about 2–3 years is discernable, which is in phase variation with IMR through the summer. The east-westward expansion of the Tibetan High combined with the westward shift of the Pacific High is responsible for the wet years in this Region. The precipitation of this region seems to be closely related to the fluctuations of the monsoon and the atmosphere/ocean interaction system with the 2–3 year period (Yasunari, 1990; Shen and Lau, 1995, *etc.*).

3) The summertime precipitation over the southeastern part of Mongolia to North China (Region III) shows a significant decreasing trend after 1955.

4) The interannual variation of JJA precipitation over the Junggar Basin (the north of the Tianshan Mountains, Region IV) shows decadal-scale oscillation. August precipitation shows significant positive correlation with IMR.

5) Though JJA precipitation over the northern part of Mongolia does not show any periodic fluctuation or trend, the July precipitation appears to be negatively correlated with IMR.

The present results have shown that the relationships of interannual variations of summer precipitation to those of general circulation fields are quite different among the sub-regions as discussed here. It should be noted that the arid/semi-arid regions in China and Mongolia are located around the confluent region of the mid-latitude westerly jet and the monsoon flow from the southwest. Thus, even if the sub-regions are located very close to each other within the study area, the interannual variation of summer precipitation in each sub-region has proved to be affected by the remarkably different general circulation systems, which are likely to interact with the complex geographical and orographical conditions.

To understand the mechanism of interannual variation of summer precipitation over this arid/semiarid region more in detail, further analyses are to be undertaken of daily and intra-seasonal variations of precipitation and associated atmospheric circulation fields, since sporadic heavy precipitation within a few days tends to determine the annual total amount of the region in question.

It is intriguing that a negative correlation is seen between the time series of precipitation over the Taklimakan Desert and IMR. These two regions are located in the opposite sides of the Tibetan Plateau. Recent studies with the general circulation models

show that the Tibetan Plateau plays a decisive role in the formation of the deserts in the mid-latitudes (Broccoli and Manabe, 1992; Kitoh, 1993), as well as the South Asian Monsoon (*e.g.*, Hahn and Manabe, 1975). The present result may imply that these roles of the Tibetan Plateau are valid also for the interannual variability of precipitation in the desert and the south Asian monsoon regions.

Acknowledgments

The authors acknowledge Dr. K. Kato, Institute for Hydrospheric-Atmospheric Sciences, Nagoya University, for constructive comments in the revision of this paper. We thank Dr. M. Nishimori, University of Tsukuba, for helpful comments in performing the rotated empirical orthogonal function analysis procedure. We appreciate Dr. A. Tsunekawa, National Institute for Environmental Studies, for fruitful discussion and information on desertification. Part of this work was supported by the research fund for science promotion from Science and Technology Agency and the grant-in-aid for scientific research from the Ministry of Education, Science and Culture in Japan.

Appendix

Geographical features of the study area

Figure A1 depicts the geographical (topographical) features over the arid/semi-arid regions of China and Mongolia related to this study. This map was drawn with reference to The Map Publisher of China (1984) and Heibonsha (1991).

References

Broccoli, A.J. and S. Manabe, 1992: The effects of orography on midlatitude Northern Hemisphere dry climates. *J. Climate*, **5**, 1181–1201.

Chen, L.-X., Y.-N. Shao, M. Dong, Z.-H. Ren and G.-S. Tian, 1991: Preliminary analysis of climate variation during the last 39 years in China, *Adv. Atmos. Sci.*, **8**, 279–288.

Chen, L.-X., M. Dong and Y.-N. Shao, 1992: The characteristics of interannual variations of the East Asian Monsoon. *J. Meteor. Soc. Japan*, **70**, 397–421.

Gadgil, S. and Joshi, N.V., 1983: Climatic clusters of the Indian region. *J. Climatol.*, **3**, 47–63.

Guo, Q.-Y. and J. Wang, 1988: A comparative study on summer monsoon in China and India. *J. Tropical Meteorol.*, **4**, 53–60 (in Chinese with English abstract).

Hahn, D.G. and S. Manabe, 1975: The role of mountains in the South Asian monsoon circulation. *J. Atmos. Sci.*, **32**, 1515–1541.

Heibonsha, 1991: *World atlas*, 205pp, (in Japanese).

Horel, J.D., 1981: A rotated principal component analysis of the interannual variability of the Northern Hemisphere 500 mb height field. *Mon. Wea. Rev.*, **109**, 2080–2092.

Kitoh, A., 1994: Modeling and observational study of the Gobi and Taklimakan Desert climate. *Proc. Intern. Symp. HEIFE, Kyoto Univ.*, 62–67.

Kripalani, R.H. and S.V. Singh, 1993: Large scale aspects of India-China summer monsoon rainfall. *Adv. Atmos. Sci.*, **10**, 71–84.

Ladd, J.W. and D.W. Driscoll, 1980: A comparison of objective and subjective means of weather typing: An example from western Texas., *J. Appl. Meteor.*, **19**, 691–704.

Lau, K.M., 1992: East Asian summer monsoon rainfall variability and climate teleconnection. *J. Meteor. Soc. Japan*, **70**, 211–242.

Murata, A., 1990: Regionality and periodicity observed in rainfall variations of the Baiu season over Japan., *Int. J. Climatol.*, **10**, 627–646.

Nishimori, M., 1994: Interannual variation of regional precipitation in Japan and its association to the atmospheric circulation in the East Asia and Northern Hemisphere. Ph. D. Thesis, University of Tsukuba, 155pp.

Parthasarathy, B., A.A. Munot and D.R. Kothawale, 1994: All-India monthly and seasonal rainfall series: 1871–1993. *Theor. Appl. Climatol.*, **49**, 217–224.

Raman, C.R.V. and Y.P. Rao, 1981: Blocking highs over Asia and monsoon droughts over India. *Nature*, **289**, 271–273.

Richman, M.B. and P.J. Lamb, 1985: Climatic pattern analysis of three- and seven-day summer rainfall in the central United States: Some methodological considerations and a regionalization. *J. Clim. Appl. Meteorol.*, **24**, 1325–1343.

Richman, M.B., 1986: Rotation of principal components. *J. Climatol.*, **6**, 293–33.

Shen, S. and K.M. Lau, 1995: Biennial oscillation associated with the East Asian summer monsoon and tropical sea surface temperature. *J. Meteor. Soc. Japan*, **73**, 105–123.

Tanaka, M., 1982: Interannual fluctuations of the tropical easterly jet and the summer monsoon in the Asian region. *J. Meteor. Soc. Japan*, **60**, 865–875.

Tanaka, M., 1983: Interaction between the active-break cycle of the summer monsoon and the circulation in Eurasia and the western Pacific. *J. Meteor. Soc. Japan*, **61**, 455–463.

The Map Publisher of China, 1984: *Atlas of physical geography of China* , 200pp, (in Chinese).

Tian, S.F. and T. Yasunari, 1992: Time space structure of interannual variations in summer rainfall over China, *J. Meteor. Soc. Japan*, **70**, 585–596.

UNEP, 1992: *World Atlas of Desertification*, Edward Arnold, 70pp.

Wang W.-C. and K. Li, 1990: Precipitation fluctuation over semi arid region in Northern China and the relationship with El Niño/Southern Oscillation. *J. Climate*, **3**, 769–783.

Walker, G.T. and E.W. Bliss, 1932: World Weather V. *Mem. Roy. Meteor. Soc.*, **4**, 53–84.

Yasunari, T., 1986: Low-frequency interactions between the summer monsoon and the northern hemisphere westerlies. *J. Meteor. Soc. Japan*, **64**, 693–708.

Yasunari, T., 1990: Impact of Indian monsoon on the

coupled atmosphere/ocean system in the tropical Pacific. *Meteor & Atmos. Phys.*, **44**, 29–41.

Yatagai, A. and T. Yasunari, 1994: Trends and decadal-scale fluctuations of surface air temperature and precipitation over China and Mongolia during the recent 40 year period (1951-1990). *J. Meteor. Soc. Japan*, **72**, 937–957.

Yoshino,M., 1994: Atmospheric circulation in the arid and semi-arid region in China. Proc. Intern. Symp. HEIFE, Kyoto Univ.Nov. 8–11, 1993, 39–50.

Yoshino, M. and T. Aoki, 1986: Interannual variations of summer precipitation in East Asia: Their regionality, recent trend, and relation to sea-surface temperature over the North Pacific. *Erdkunde* (*Bonn*), **40**, 94–104.

Yoshino, M.M. and M. Chiba, 1984: Regional division of China by precipitation and its annual variation type. *Geogr. Rev. Japan*, **57A**, 583–590. (in Japanese with English abstract).

中国とモンゴルの乾燥・半乾燥地域における夏季降水量の経年変動：その地域性とアジアの夏季モンスーンとの関係

谷貝田亜紀代[1]
(筑波大学地球科学研究科)
安成哲三
(筑波大学地球科学系)

中国とモンゴルの乾燥・半乾燥地域における夏季降水量の経年変動を解析した。回転主成分分析の手法を夏季 (6–8 月) 降水量時系列 (1951–1990 年) に適用し、その経年変動特性により、対象地域を次の 5 地域に区分することが出来た。I) タクラマカン砂漠、II) 黄土高原、III) 中国華北～モンゴル中・南東部、IV) 天山山脈の北側、V) モンゴル北部。地域 III) の代表的な時系列は、1955 年以降の降水量の有意な減少傾向を示した。

次に、対象地域の降水量の経年変動とアジアモンスーン活動との関連を調べるために、インド総降水量資料とこれらの地域の降水量変動との関係をモンスーン期の合計降水量についてだけでなく、夏季の各月について調べた。その結果、地域 I)、II) の代表時系列はインド総降水量と、それぞれ負、正の相関が見られたことから、ここではこの 2 地域の夏季降水量の経年変動と大気大循環場との関連を、北半球の 100 hPa、500 hPa 高度及び地上気圧の偏差を使用して解析した。

その結果、地域 I) (タクラマカン砂漠) の夏季降水量の経年変動は、偏西風循環の風上側 (大西洋～ユーラシア大陸) の偏差と関係し、多雨年にはトラフが 90°E 付近に存在すること、また、チベット高気圧が多 (小) 雨年にはその東側で強く (弱く) なることがわかった。地域 I) の 6、7 月の降水量はインド総降水量と負相関が見られた。この両地域の夏季降水量の経年変動の関係は中央アジア周辺の比較的局地的な循環場を介在していることが示唆された。

一方、地域 II) (黄土高原) の 2–3 年周期を呈する時系列は、6–9 月の各月においてインド総降水量と正相関が見られた。対応する大循環場の変動は、太平洋高気圧、チベット高気圧、イラン周辺の地上気圧に見られた。これらは地域 II) の夏季降水量の経年変動が、よりグローバルな、モンスーンに伴う大気海洋相互作用と密接な関わりがあることを示唆している。

[1]現所属：宇宙開発事業団　地球観測データ解析研究センター